Mutations in UDP-Glucose:Sterol Glucosyltransferase in Arabidopsis Cause Transparent Testa Phenotype and Suberization Defect in Seeds[1][C][W][OA]

Seth DeBolt*, Wolf-Rüdiger Scheible, Kathrin Schrick, Manfred Auer, Fred Beisson, Volker Bischoff, Pierrette Bouvier-Navé, Andrew Carroll, Kian Hematy, Yonghua Li, Jennifer Milne, Meera Nair, Hubert Schaller, Marcin Zemla, and Chris Somerville

Department of Horticulture, University of Kentucky, Lexington, Kentucky 40506 (S.D., M.N.); Max Planck Institute of Molecular Plant Physiology, Science Park Golm, 14476 Potsdam, Germany (W.-R.S., V.B.); Keck Graduate Institute of Applied Life Sciences, Claremont, California 91711 (K.S.); Division of Biology, California Institute of Technology, Pasadena, California 91125 (K.S.); Division of Biology, Kansas State University, Manhattan, Kansas 66506 (K.S.); Lawrence Berkeley National Laboratory, Berkeley, California 94720 (M.A., M.Z.); Membrane Biogenesis Laboratory (UMR 5200), Centre National de la Recherche Scientifique-University of Bordeaux 2, 33076 Bordeaux cedex, France (F.B., Y.L.); Institute for Plant Molecular Biology, Unite Propre de Recherche Centre National de la Recherche Scientifique 2357, 67083 Strasbourg, France (P.B.-N., H.S.); Department of Biology (A.C.) and Global Climate and Energy Project (J.M.), Stanford University, Stanford, California 94305; and Energy Biosciences Institute, University of California, Berkeley, California 94720 (K.H., C.S.)

In higher plants, the most abundant sterol derivatives are steryl glycosides (SGs) and acyl SGs. Arabidopsis (*Arabidopsis thaliana*) contains two genes, *UGT80A2* and *UGT80B1*, that encode UDP-Glc:sterol glycosyltransferases, enzymes that catalyze the synthesis of SGs. Lines having mutations in *UGT80A2*, *UGT80B1*, or both *UGT80A2* and *UGT8B1* were identified and characterized. The *ugt80A2* lines were viable and exhibited relatively minor effects on plant growth. Conversely, *ugt80B1* mutants displayed an array of phenotypes that were pronounced in the embryo and seed. Most notable was the finding that *ugt80B1* was allelic to *transparent testa15* and displayed a transparent testa phenotype and a reduction in seed size. In addition to the role of *UGT80B1* in the deposition of flavanoids, a loss of suberization of the seed was apparent in *ugt80B1* by the lack of autofluorescence at the hilum region. Moreover, in *ugt80B1*, scanning and transmission electron microscopy reveals that the outer integument of the seed coat lost the electron-dense cuticle layer at its surface and displayed altered cell morphology. Gas chromatography coupled with mass spectrometry of lipid polyester monomers confirmed a drastic decrease in aliphatic suberin and cutin-like polymers that was associated with an inability to limit tetrazolium salt uptake. The findings suggest a membrane function for SGs and acyl SGs in trafficking of lipid polyester precursors. An ancillary observation was that cellulose biosynthesis was unaffected in the double mutant, inconsistent with a predicted role for SGs in priming cellulose synthesis.

Steryl glycosides (SGs) and acyl SGs (ASGs) are abundant constituents of the membranes of higher plants (Frasch and Grunwald, 1976; Warnecke and Heinz, 1994; Warnecke et al., 1997, 1999). SGs are synthesized by membrane-bound UDP-Glc:sterol glucosyltransferase (Hartmann-Bouillon and Benveniste, 1978; Ury et al., 1989; Warnecke et al., 1997), which catalyzes the glycosylation of the 3β-hydroxy group of sterols to produce a 3-β-D-glycoside. UGT80A2 has been found in the plasma membrane, Golgi vesicles, the endoplasmic reticulum membrane, and occasionally the tonoplast (Hartmann-Bouillon and Benveniste, 1978; Yoshida and Uemura, 1986; Ullmann et al., 1987; Warnecke et al., 1997). It has also been reported that a UDP-Glc-dependent glucosylceramide synthase from cotton (*Gossypium hirsutum*) is capable of synthesizing SG in plants (Hillig et al., 2003). All plant sterols can be glycosylated, given that sterol substrates are pathway end products (Δ^5-sterols in Arabidopsis [*Arabidopsis thaliana*]) and not intermediates. The most commonly observed glycoside is Glc (Warnecke et al., 1997) but Xyl (Iribarren and Pomilio, 1985), Gal, and Man have been observed (Grunwald, 1978). Although rare in

[1] This work was supported by grants from the Balzan Foundation and the U.S. Department of Energy (grant no. DE–FG02–09ER16008 to C.S. and grant no. NSF:IOS–0922947 to S.D.). K.S. was supported by the U.S. Department of Agriculture (grant no. USDA:2007–35304–18453) and the National Science Foundation (grant no. NSF:MCB–051778).

* Corresponding author; e-mail sdebo2@email.uky.edu.

The author responsible for distribution of materials integral to the findings presented in this article in accordance with the policy described in the Instructions for Authors (www.plantphysiol.org) is: Seth DeBolt (sdebo2@email.uky.edu).

[C] Some figures in this article are displayed in color online but in black and white in the print edition.

[W] The online version of this article contains Web-only data.

[OA] Open access articles can be viewed online without a subscription.

www.plantphysiol.org/cgi/doi/10.1104/pp.109.140582

occurrence, SGs with di-, tri-, and tetraglucoside residues have also been reported (Kojima et al., 1989). SGs can be acylated, polyhydroxylated, or sulfated, but ASGs with fatty acids esterified to the primary alcohol group of the carbohydrate unit are the most common modifications (Lepage, 1964).

SGs have been found as abundant membrane components in many species of plants, mosses, bacteria, fungi, and in some species of animals (Esders and Light, 1972; Mayberry and Smith, 1983; Murakami-Murofushi et al., 1987; Haque et al., 1996), yet relatively little is known about their biological functions. Because of the importance of sterols in membrane fluidity and permeability (Warnecke and Heinz, 1994; Warnecke et al., 1999; Schaller, 2003) and the phospholipid dependence of UDP-Glc:sterol glucosyltransferase (Bouvier-Nave et al., 1984), it has been postulated that SGs may have a role in adaptation to temperature stress (Palta et al., 1993). A difference in the proportion of glycosylated versus acylated sterols were reported in two different solanaceous species under the same cold acclimation experiment (Palta et al., 1993). In one species an increase in SG was correlated with a decrease in ASG. In contrast, the other species displayed no change in SG and ASG levels with cold acclimation conditioning. Hence, evidence for a role in temperature adaptation is lacking.

Understanding the processes involved in SG production has additional human importance because SGs are highly bioactive food components and laboratory mice fed SGs faithfully lead to either amyotrophic lateral sclerosis or parkinsonism pathologies (Ly et al., 2007). Similarly, consumption of seeds of the cycad palm (*Cycas micronesica*), containing high SG levels, has been linked to an unusual human neurological disorder, amyotrophic lateral sclerosis-parkinsonism dementia complex, in studies of the people of Guam (Cruz-Aguado and Shaw, 2009). However, SG is a dominant moiety of all plant membranes and some of the most widely consumed plant products in the United States such as soybeans (*Glycine max*) have concentrations well within the dose range obtained by consumption of cycad seeds. Cholesterol glycoside is the SG most commonly identified in animal membranes and is exemplified by cases in snake epidermis cells (Abraham et al., 1987) and human fibroblast cells under heat shock (Kunimoto et al., 2000). Regarding a role for SGs in the membrane, in comparison to normal sterols, SG and ASG exchange more slowly between the monolayer halves of a bilayer, which could serve to regulate free sterol (FS) content and its distribution (Ullmann et al., 1987; Warnecke et al., 1999).

A study of cellulose synthesis in herbicide-treated cotton fibers found that sitosterol β-glucoside (SSG) copurified with cellulose fragments (Peng et al., 2002), leading to speculation that SGs act as a primer for cellulose biosynthesis in higher plants (Peng et al., 2002). In support of the hypothesis, SSG biosynthesis was reported to be pharmacologically inhibited by the known cellulose biosynthesis inhibitor 2-6-dichlorobenzonitrile (DCB; Peng et al., 2002). However, in subsequent studies, DCB inhibition of cellulose synthesis was not reversed by the exogenous addition of SSG, and the effects of DCB on cellulose synthesis were so rapid that the turnover of SGs would need to be very fast to account for the effects of DCB on cellulose synthesis (DeBolt et al., 2007). Schrick et al. (2004) reported that sterol biosynthesis mutants *fackel*, *hydra1*, and *sterol methyltransferase1/cephalopod* have reduced levels of cellulose but a specific effect on SGs was not established. Hence, a role for SGs in plant growth and development remains speculative.

Here we describe a genetic analysis of the biological roles of two isoforms of UDP-Glc:sterol glucosyltransferase, UGT80A2 and USGT80B1, that participate in the synthesis of SG in Arabidopsis. UDP-Glc-dependent glucosylceramide synthase may also be capable of synthesizing SG in plants (Hillig et al., 2003), but no analysis was performed herein. We show that mutations in one of these genes, *UGT80B1*, results in a lack of flavanoid accumulation in the seed coat and that it corresponds to *transparent testa15* (*tt15*). Analysis of *ugt80A2*, *ugt80B1*, and a double mutant suggests that glycosylation of sterols by the UGT80A2 and UGT80B1 enzymes had no measurable consequence on cellulose levels in Arabidopsis seed, siliques, flowers, stems, trichomes, and leaves. Rather, we demonstrate that mutation of *UGT80B1* principally alters embryonic development and seed suberin accumulation and cutin formation in the seed coat, leading to abnormal permeability and tetrazolium salt uptake.

RESULTS

Isolation of T-DNA Mutations in the Genes Encoding UDP-Glc:Sterol Glucosyltransferase

Warnecke et al. (1999) previously reported the isolation of a cDNA coding for UDP-Glc:sterol glucosyltransferase from Arabidopsis. The gene they described, At3g07020, which we designate here as *UGT80A2*, encodes a 637-amino acid protein comprised of 14 exons and 13 introns. The completion of the Arabidopsis genome sequence revealed the existence of a second unlinked gene, At1g43620, encoding a 615-amino acid protein and corresponding to a genomic region encompassing 14 exons and 13 introns, as well as a predicted intron in the 3′ untranslated region. The predicted gene product that we designate as *UGT80B1* exhibits strong sequence identity to *UGT80A2* (61.5% and 51.2% amino acid similarity and identity, respectively).

T-DNA insertion alleles for both *UGT80A2* and *UGT80B1* were identified by screening the University of Wisconsin T-DNA collection (Sussman et al., 2000). Homozygous lines carrying T-DNA mutations in *UGT80A2* and *UGT80B1* were confirmed by PCR (Supplemental Fig. S1). A double mutant homozygous for both the *ugt80* (*B1* and *A2*) mutations was obtained by crossing *ugt80A2* and *ugt80B1* homozygous plants,

followed by PCR screening of the F_2 population for the double homozygote. The double mutant was found to be viable and was designated *ugt80A2,B1*.

Sterol and Sterol-Derivative Analysis Reveals Reduced Levels of SG and ASG and Increased FSs in the *ugt80A2,B1* Mutant

FSs, steryl esters (SEs), SG, and ASG were isolated from leaf tissue of wild-type, *ugt80A2*, and *ugt80B1* mutants, and the *ugt80A2,B1* double mutant. The wild-type tissues contained FS, SG, and ASG, at levels that are similar to those previously described (Patterson et al., 1993). There was no difference in FS + SE content between wild type and *ugt80A2,B1* in leaf or stem tissue (Fig. 1A). However, in inflorescence + silique tissue FS + SE content was 26% higher in *ugt80A2,B1* relative to wild type (Fig. 1A). SG + ASG content decreased 5-, 21-, and 22-fold in leaf, stem, and siliques + inflorescence tissue, respectively (Fig. 1B). Sterol derivatives that were SG + ASG were significantly reduced in *ugt80A2* and *ugt80B1* mutants (Supplemental Table S1). The ratio of SG + ASG:FS (%) for rosette leaf tissue and ASG:SE (%) for stem and inflorescence tissue both showed additive alteration in the sterol profile between the single and double mutant (Supplemental Table S1). Thus, both *UGT80A2* and *UGT80B1* are required for the normal production of SG and ASG, and their gene products appear to function in a partially redundant manner in catalyzing the glycosylation of 24-alkyl-Δ^5-sterols in Arabidopsis.

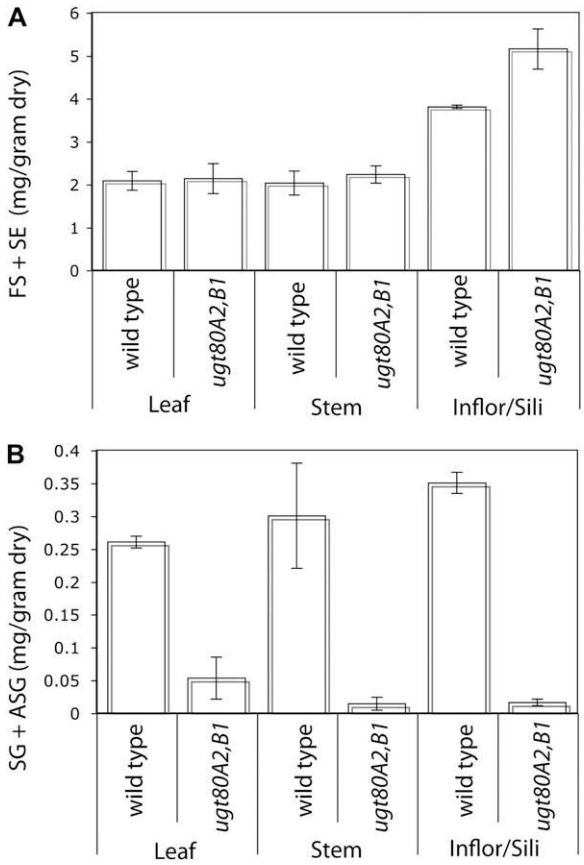

Figure 1. Analysis of sterols and sterol derivates in *ugt80A2,B1* mutant relative to wild type. Total sterol derivatives were quantified and compared between wild-type and mutant plants in mg per gram dry weight^{-1} as FS + SE (A) and SG + ASG (B). FS + SE was the sum of FS measured by GC-FID + sterols measured by GC-FID released from SE fraction after saponification. Values are the mean of three replicates and experimental analysis was duplicated; error bars indicate SE from the mean. Inflor/Sili, Inflorescence/silique.

SG Mutant *ugt80A2,B1* Exhibits a Slow Growth Phenotype and Elongation Defects in Embryogenesis

The mature *ugt80A2*, *ugt80B1*, and double-mutant plants were viable and fully fertile. At 22°C the growth habit of the mature plants showed no substantial radial swelling or dwarfing as was expected for a cellulose-deficient mutant. Because of evidence suggesting that SG may be important in stress responses in fungi (Warnecke et al., 1999), slime molds (Murakami-Murofushi et al., 1987), and plants (Patterson et al., 1993), we grew the mutants at the seedling stage at a range of temperatures from 10°C to 22°C. The results indicated significantly lower seedling growth rates in the double mutant compared to wild-type, *ugt80A2*, and *ugt80B1* single mutants at all 22°C, 15°C, and 10°C temperatures (Supplemental Fig. S2). We also explored the ability of the plants to acclimate to cold by measuring ion leakage and survival rates after 1 week acclimation at 4°C but observed no significant difference between any of the lines and wild type (Supplemental Fig. S3). Mutant and wild-type parental plants grown on soil at 4°C for 5 months in 24-h light also displayed no differences in height or growth habit of the plants (data not shown).

Since double mutants displayed a slow growth phenotype during postembryonic stages, we asked whether growth during embryogenesis was also affected. Embryonic stages of development were compared between the wild type and double mutant (Fig. 2). Although the early stages of double-mutant development, from globular to young heart stages, displayed morphologies that were similar to wild type, the late heart, torpedo, bent-cotyledon, and mature embryo stages exhibited abnormally stunted morphologies, indicating a defect in cell elongation (Fig. 2). Elongation of the cotyledon primordia, developing hypocotyl, and embryonic root were affected.

Cellulose and Cell Wall Sugar Levels Are Not Significantly Altered in SG Mutants

The cellulose priming model (Peng et al., 2002) predicts that a deficiency in SG may alter cellulose synthesis. To test this hypothesis we measured the relative amounts of crystalline Glc derived from cellulose in flowers, siliques, leaves, trichomes, and stems

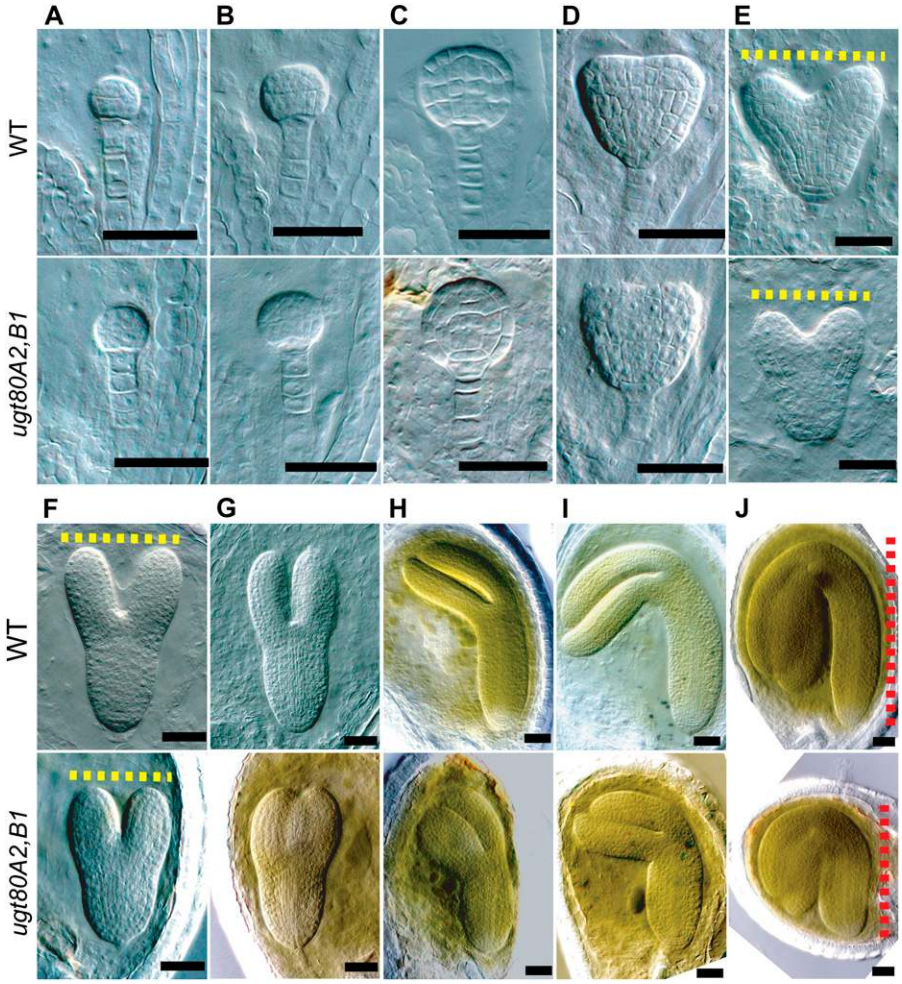

Figure 2. Elongation defects in *ugt80A2,B1* double-mutant embryos. Nomarski images of embryogenesis during globular (A–C), heart (D and E), torpedo (F and G), bent-cotyledon (H and I), and mature embryo (J) stages. Each vertical section exhibits the identical scale so that the sizes of the mutant embryos can be directly compared with that of wild type (WT; top row). Deviations from the wild-type morphology are first apparent at the late heart stage (F). The *ugt80A2,B1* mutant displays elongation defects in outgrowth of the cotyledon primordia (yellow dotted lines). Elongation defects along the apical-basal axis are more obvious in the torpedo, bent-cotyledon, and mature stages. Red dotted lines indicate shorter hypocotyl and root lengths for *ugt80A2,B1* at the mature embryo stage (J). Bars = 50 μm. [See online article for color version of this figure.]

of the double mutant. The results of these measurements indicated no significant difference in the amount of cellulose in the mutants in comparison with wild-type plants in any of our experiments (Fig. 3A). Cellulose measurements were performed on leaf trichomes using birefringence and the results also failed to uncover a deficiency in cellulose content in the double mutant as did Fourier transform infrared analysis (data not shown). Neutral sugar analysis showed some minor differences in the sugar profile of the cell wall (Fig. 3B). Specifically, in the *ugt80B1* mutant Xyl, Man, and Glc content appeared greater than that of the wild-type plant and the *ugt80A2* had slightly greater Glc levels than wild type.

Promoter::GUS Fusions Indicate Distinct But Partially Overlapping Relative Gene Expression Patterns for *UGT80A2* and *UGT80B1*

To investigate *UGT80A2* and *UGT80B1* expression in more detail, we constructed transgenic plants in which the GUS reporter gene was placed under the control of the approximately 2-kb promoter regions upstream of the *UGT80A2* and *UGT80B1* genes. Relative gene expression of *proUGT80A2*::*GUS* was observed in a patchy distribution in cauline leaf epidermal cells, stomata, pollen, around the base of siliques and in the stamen (Supplemental Fig. S4). Relative gene expression of *proUGT80B1*::*GUS* was primarily observed in leaves, seedlings, around the apical tip of cotyledons, and developing seeds (Supplemental Fig. S5). Characterization of the GUS staining pattern in embryos revealed that expression was strongest around the apical tip of the cotyledons and at the root apex. Strong GUS expression was also apparent around the seed coat epidermal cell boundaries and in the central columella, but not in the trough (Supplemental Fig. S5). Taken together the results indicate that *UGT80A2* and *UGT80B1* mRNAs are found in distinct expression domains within the plant. *UGT80B1* was uniquely expressed in the seed coat and in the cotyledons of the embryo, consistent with its mutant phenotype related to these tissues. The promoter fusion expression results for both genes are largely consistent with expression analysis performed using available microarray data for Arabidopsis

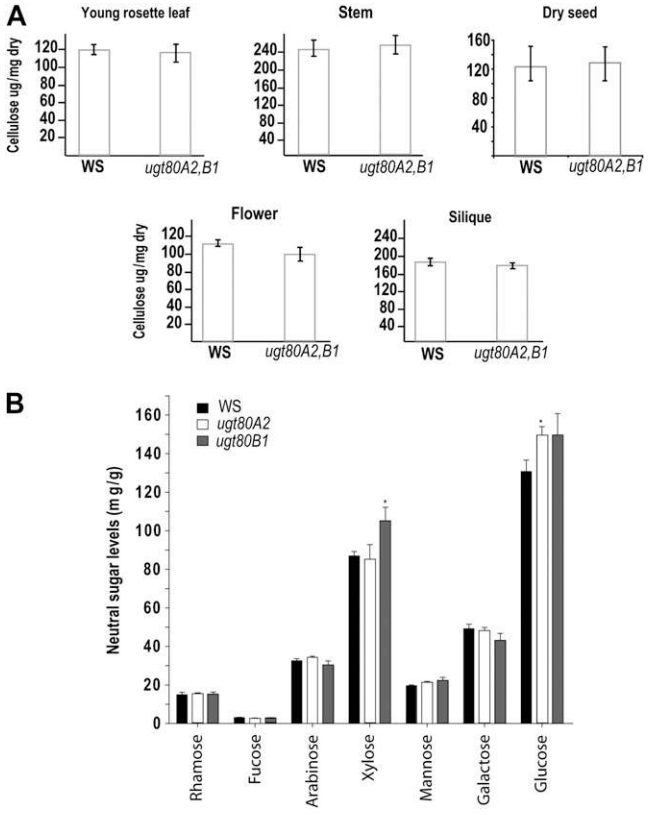

Figure 3. Cellulose and cell wall analysis. A, Cellulose composition was measured for wild-type WS-O and double mutant in various tissues. B, Cell wall neutral sugar composition of the *ugt80A2* and *ugt80B1* single mutants was analyzed and compared with that of wild-type WS-O plants.

(available online through The Arabidopsis Information Resource; https://3.met.genevestigator.com/).

Mutations in *UGT80A2* and *USG80B1* Genes Result in Reduced Seed Size, Transparent Testa, and Salt Uptake Phenotypes

Visual inspection revealed a lightened seed coat hue in *ugt80B1* and in the double mutant as well as a dramatic reduction in seed size compared to wild type (Fig. 4A; Supplemental Fig. S6). The light-colored testa phenotype in the *UGT80B1* mutant was consistent with being a *transparent testa* mutant and this was confirmed by allelism tests to *tt15* (data not shown; Focks et al., 1999). The color of seed from *ugt80A2* mutants did not appear lightened to the same degree as *ugt80B1*, however *ugt80A2* seeds displayed a measurable reduction in size (Fig. 4A; Supplemental Fig. S6).

A series of histochemical and microscopy analyses were performed to deduce possible reasons for the increased permeability of the *ugt80B1* mutant. When seeds were incubated in a solution of tetrazolium salts, *ugt80B1* and the double-mutant seed were found to be highly sensitive to salt uptake (Fig. 4B). Wild-type and *ugt80A2* seeds absorbed small amount of salt at the hilum region, but *ugt80B1* seeds were unable to limit uptake and the entire embryo became stained with formazan dye (a tetrazolium reduction product; Fig. 4B). The salt-uptake phenotype of *ugt80B1* mutants was rescued by complementation with a *p35S::UGT80B1* construct (Fig. 4B). Additional salt-uptake experiments were performed during the development of the embryo within the seed. Wild-type seeds restricted salt uptake during the maturation stages, whereas double mutants never developed the ability to restrict salt from penetrating the seed coat (data not shown).

Pigmentation of the seed coat was determined by the deposition of flavanoids using 4-(dimethylamino)-cinnamaldehyde (DMACA) reagent. Consistent with the transparent testa phenotype, the most drastic reduction in DMACA staining was in *ugt80B1* and in the double mutant (Fig. 4C). The DMACA staining phenotype of *ugt80B1* mutants was also rescued by complementation with a *p35S::UGT80B1* construct (Fig. 4C).

Flavanol and Starch Analysis in the Seedling Reveals Altered Cotyledon Morphology and Hydathode Composition in *ugt80B1* Mutants

Seedlings were grown in the dark for 3 d and then stained with diphenylboric acid 2-aminoethyl ester (DPBA) to reveal sinapate derivatives. In comparison to wild type, the *ugt80B1* mutant displayed a striking increase in sinapate derivatives (blue color) localized specifically at the apical hydathode in the cotyledon (Supplemental Fig. S7A). The double mutant did not show a substantial change from the *ugt80B1* single mutant in the DPBA staining pattern at the hydathode.

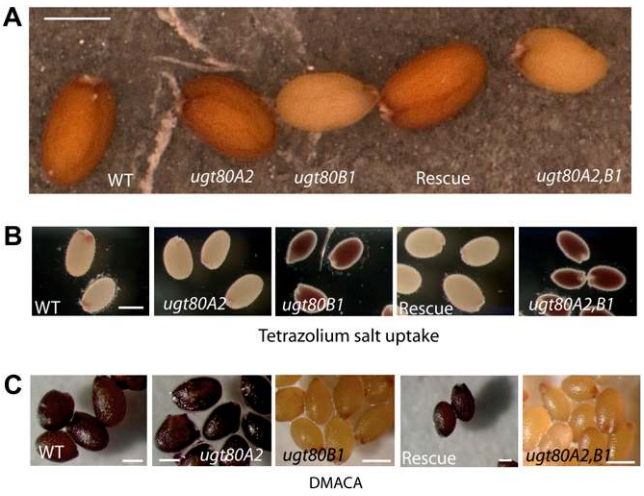

Figure 4. Transparent testa phenotype of *ugt80B1* and *ugt80A2,B1* mutants. A, Light microscopy to visualize seed coloration in wild type (WT), *ugt80A2*, *ugt80B1*, *rescue*, and *ugt80A2,B1*. B, Tetrazolium red uptake in wild type, *ugt80A2*, *ugt80B1*, *rescue*, and *ugt80A2,B1*. C, DMACA staining shows altered flavanol composition in wild type, *ugt80A2*, *ugt80B1*, *rescue*, and *ugt80A2,B1* (scale bars = 150 μm).

After 2 d of dark growth, wild-type seedlings exhibited blue-colored sinapate derivatives that were only localized at the hydathode region whereas in *ugt80B1* and the double mutant, almost half the cotyledon showed sinapate derivatives. Thus, it appears that the accumulation of sinapate derivatives around the hydathode of cotyledons is a natural occurrence in seedling development and that *ugt80B1* mutants retain this pattern in a greater proportion of the cotyledon during development. The cotyledon hydathode from *ugt80A1,B2* seedlings was stained with an iodine mixture (I2:KI) to determine whether starch accumulation is altered in this region. Reminiscent of the DPBA staining (Supplemental Fig. S7B), the double-mutant cotyledon displayed a distinct staining pattern around the hydathode region that was markedly more pronounced than wild-type hydathode staining. High-magnification imaging of the hydathode region revealed an altered morphology of cells in this region in double-mutant seedlings.

SGs Are Critical for Normal Cell Morphology of the Seed Coat and Deposition of Lipid Polyesters as Analyzed by Electron Microscopy and Gas Chromatography-Mass Spectrometry

Scanning electron microscopy (SEM) was applied to ascertain possible alterations in the morphology of cells within the seed epidermis (Fig. 5, A–D). Severe defects in cell morphology were evident in double-mutant seed (Fig. 5, B–D). In addition to smaller seed size, approximately one-third of seed displayed a sunken region extending from the hilum (Fig. 5B). Further examination by transmission electron microscopy (TEM) was performed to visualize the ultrastructure of the seed coat in the mutants. Strikingly, the electron-dense outer layer covering the wild-type seed coat was found to be absent in *ugt80B1* and double mutant (Fig. 5, E and F). To understand the changes in development, the same analysis was applied at the developmental stage when wild-type seeds can first repel tetrazolium salts. At this stage wild-type seed already displayed an electron-dense cuticle layer covering the seed coat, and were beginning to form columella. By contrast, the cuticle layer was greatly diminished in the double mutant, and the columella were less prominent (Fig. 5D). The cellular morphology in the mutant was strikingly different from wild type: Aberrant dispersed electron-dense regions that are observed in the cytosol may represent an abnormal accumulation of suberin, wax, or cutin that failed to be transported to the outer surface of the seed. The failure to form columella was consistent with the SEM data (Fig. 5D) and indicates that this defect arose during embryonic development (Fig. 2).

Next, we examined the hilum region of the wild-type seed compared with mutant by autofluorescence analysis using a broad-spectrum UV light source, since autofluorescence around the hilum reflects accumulation of suberin (Beisson et al., 2007). The results

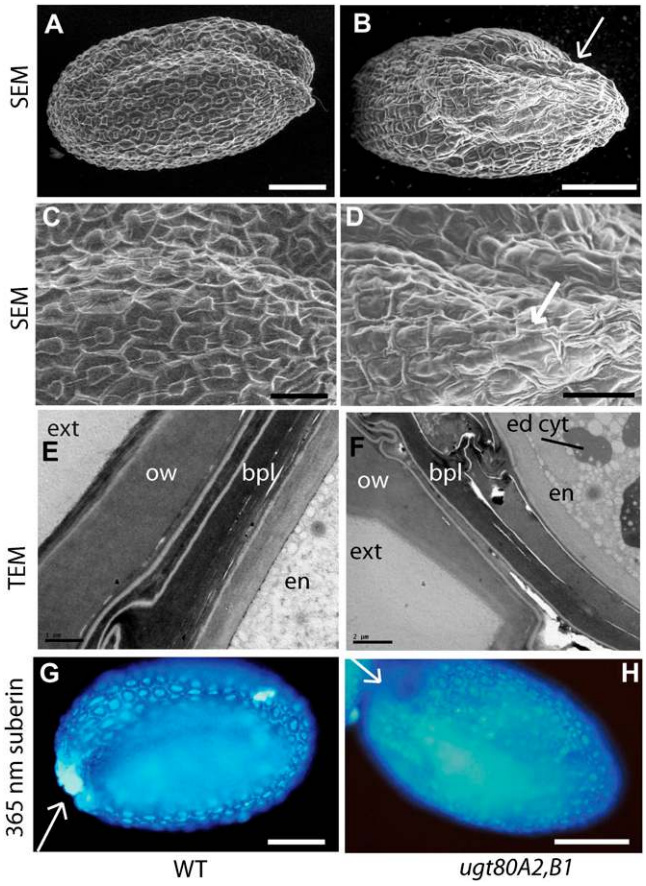

Figure 5. Scanning and transmission electron micrographs and suberin assessment of seed phenotype indicate aberrant lipid polyester production. A and C, Wild-type (WT) seeds exhibit uniform cell shapes and well-formed columella. B and D, Double-mutant seed with a collapsed region of the seed near the funiculus. Columella exhibit aberrant morphology (scale bar in A and B = 100 μm; C and D = 15 μm). E, TEM micrograph of the outer layer of a mature wild-type seed. An electron-dense cuticle covers the outer seed coat. The integuments have collapsed into a dense brown pigment layer. F, Micrograph of double-mutant seed at maturity. The electron-dense cuticle layer is absent (arrow; scale bar = 1 μm). G and H, Suberin autofluorescence in wild-type seeds (G) by illumination under 365-nm UV light compared with the *ugt80B1* mutant (H), which lacks suberin accumulation (arrows; scale as in A and B). bpl, Brown pigment layer; ed cyt, electron dense regions in the cytoplasm; en, endosperm; ext, exterior; ow, outer cell wall. [See online article for color version of this figure.]

indicate that the hilum region of both the *ugt80B1* and double mutant exhibit reduced suberization, which appears as a bright autofluorescent signal in *ugt80A2* and wild-type seed (Fig. 5, G and H). Consistent with these observations, analysis of lipid polyester monomers from seeds of the *ugt80B1* mutant in comparison to wild type showed an overall 50% reduction in total aliphatics (Fig. 6). The vast majority of the 45 polyester monomers identified were significantly reduced in the *ugt80A2,B1* mutant, including the C22 and C24 very-long-chain ω-hydroxy fatty acids typical of suberin. The reduction in polyester

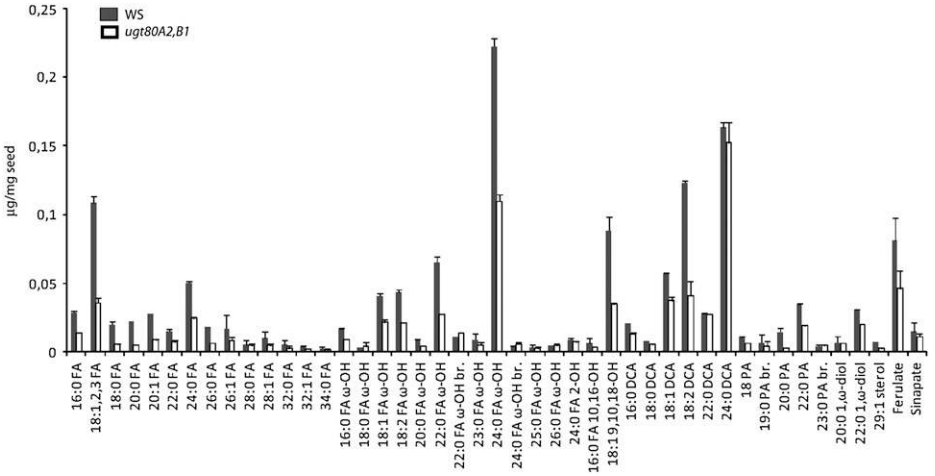

Figure 6. Lipid polyester monomers from seeds of wild-type and *ugt80A2,B1* plants. The insoluble dry residue obtained after grinding and delipidation of tissues with organic solvents was depolymerized by acid-catalyzed methanolysis and aliphatic and aromatic monomers released were analyzed by GC-MS. Values are means of four replicates. Error bars denote SDs. DCAs, Dicarboxylic acids; FAs, fatty acids; PAs, primary alcohols; br., branched.

monomers was however not equivalent. For example, the C24 ω-hydroxy fatty acid was reduced 2-fold and the C24 α,ω-diacid remained almost unchanged although both monomers are known to be mostly localized to the outer integument of the seed coat (Molina et al., 2008). Interestingly, the 9,10,18-trihydroxyoleate cutin monomer, which is largely specific to the embryo (Molina et al., 2006), was 60% reduced. This observation, together with the defects apparent in the cutin-like electron-dense layer of the seed coat surface (Fig. 5F), indicates that the deposition of cutin polymer is also affected.

DISCUSSION

Here we used a reverse-genetic approach to explore the functions of UDP-Glc:sterol glucosyltransferase in plants. T-DNA mutations in *UGT80A2* (At3g07020) and *UGT80B1* (At1g43620) were identified and characterized in addition to the corresponding double mutant. Sterol derivatives SG + ASG were significantly reduced in *ugt80A2* and *ugt80B1* single mutants (Supplemental Table S1). Hence, both UGT80A2 and UGT80B1 function in catalyzing the glycosylation of 24-alkyl-Δ^5-sterols in Arabidopsis. Moreover, FS + SE increased 26% in *ugt80A2,B1* silique + inflorescence tissue relative to wild type. In the same tissue SG + ASG content decreased 22-fold in *ugt80A2,B1* relative to wild type (Fig. 1). These data implied a feedback relationship between the FS + SE content relative to SG + ASG in certain tissues. Phenotypic examination revealed that *ugt80B1* caused the most notable phenotypes. Based on allelism tests, *ugt80B1* corresponds to the previously unannotated *tt15* mutant (Focks et al., 1999). HPLC analysis of flavanols and condensed tannins performed independently showed aberrant condensed tannin synthesis in *ugt80B1* (Isabelle Debeaujon, personal communication), confirming staining results. The accumulation of suberin around the hilum region of the wild-type Arabidopsis seed, where the funiculus dissociates the seed from the parent, was ablated in the *ugt80B1* mutant (Fig. 5, G and H). Reduction in the amount of suberin observed visually by autofluorescence was confirmed by gas chromatography-mass spectrometry (GC-MS) analysis (Fig. 6). But moreover, GC-MS analysis also revealed that many of the structurally diverse lipid polyesters such as cutin and aliphatic suberin were reduced in *ugt80A2,B1.* Thus, we propose a membrane function for SG and ASG in the trafficking of lipid polyester precursors to form suberin and cutin in the seed.

Other transparent testa mutants have been characterized by forward genetics in Arabidopsis and these fall broadly into two categories: transcription factors and genes catalytically involved in the flavanoid biosynthesis pathway (Debeaujon et al., 2003). An atypical mutation leading to a transparent testa phenotype was found to map in a gene for plasma membrane H+-ATPase (AHA10; Baxter et al., 2005). This mutation caused a 100-fold decrease in proanthocyanidins (PAs) in seed endothelial cells. The deficiency in PA in *aha10* mutants was correlated with a defect in biogenesis of a large central vacuole (Baxter et al., 2005), yet the reason for the lack of PA accumulation was not clear. Hence, like *ugt80B1*, the *aha10* mutant appears to be distinct from other transparent testa mutants that ablate catalytic functions within the flavanoid pathway. *aha10* and *ugt80B1* may represent a novel class of mutants that indirectly cause a transparent testa phenotype due to membrane-related defects. In studies with animal cells, the gradient of SG and ASG content has been correlated with membrane thickness and the sorting of membrane proteins based on the lengths of the transmembrane domains (Bretscher and Munro, 1993). Alteration of the sterols in the membrane may result in aberrant behavior of an assortment of membrane proteins. In this scenario, alterations in the physical properties of the membrane dynamics such as reduced rate of exchange of SG and ASG between the monolayer halves of a bilayer may affect some aspect of flavanoid synthesis, such as transport or accumula-

tion. Among proteins directly involved in flavanoid biosynthesis, chalcone synthase and chalcone isomerase are thought to be membrane anchored (Jez et al., 2000). Also, as-yet-unidentified proteins are presumably involved in the transport of flavanoids into vacuoles.

The sterol content of plant membranes has been observed to change in response to environmental conditions and it has been suggested that alterations in the sterol composition of the plasma membrane may play a role in the cold acclimation process (Patterson et al., 1993). Moreover, gene expression data from available microarray experiments (Genome Cluster Database) suggest that *UGT80B1* transcripts are slightly up-regulated by cold stress. The mutants described here provided an opportunity to test this hypothesis with respect to SG and ASG. We investigated the adaptive response to temperature stress but were unable to detect a significant difference between mutants and wild type. Thus, although sterol content of membranes in Arabidopsis was modulated in part by SG and ASG synthesis, loss of these membrane components did not appear to adversely affect growth or viability at low temperatures. The slightly reduced growth rate of the mutants at all temperatures indicates that SGs are important for growth and development, as might be expected from their widespread presence in plants. However, this role appears to be beneficial rather than crucial.

A significant motivation for the isolation of the *ugt80A2* and *ugt80B1* mutants was to test the postulate that SG functions in cellulose biosynthesis. The elongation defects of double-mutant embryos (Fig. 2) suggested possible defective cell wall biogenesis. Peng et al. (2002) observed the tight association of SSG with an amorphous form of cellulose and speculated that SSG may be a primer for the initiation of cellulose. We tested the hypothesis by measuring cellulose content in leaves, stems, roots, flowers, siliques, and trichomes of the double mutant but found no significant differences between mutant and wild type in cellulose content, and only minor alterations in the content of the sugars that comprise the other cell wall polysaccharides (Fig. 3, A and B). Therefore, if SSG biosynthesis by UGT80A2 or UGT80B1 has a role in cellulose biosynthesis, it was a dispensable role or was fulfilled by residual levels of SSG. The low residual level of SG in the double mutant also prevented a definitive answer to the question of whether plants require SG for viability and/or cellulose synthesis since it is possible that plants require only a trace amount of SSG. A possible source of residual SSG may arise from the activity of glucosylceramide synthase, which Hillig et al. (2003) demonstrated was capable of catalyzing the glycosylation of sterols in vitro.

Uptake of tetrazolium salt occurred far more readily in *ugt80B1* mutants, suggesting less control of seed coat permeability (Fig. 4B). A plausible explanation for the salt-uptake phenotype in the *ugt80B1* mutant may be a direct result of reduced seed coat suberization in the hilum region (Fig. 4, G and H) and/or reduced cuticle formation at the surface of the outer integument. Cutin-like monomers are also known to be present in the inner integument and in the embryo (Molina et al., 2006, 2008). Lipid polyesters (cutin, aliphatic suberin) are structurally related biopolymers that are involved in controlling water relations (Pollard et al., 2008) and seem to have conserved features in their mechanisms of biosynthesis and export to the cell wall (Li et al., 2007). However, there was no obvious explanation as to why the reduction in SG and ASG impacted hilum suberization as well as seed coat and embryo cuticle formation. Thus, we speculate that SG and ASG are necessary membrane components required for efficient lipid polyester precursor trafficking or export into the apoplast in plant seeds.

MATERIALS AND METHODS

Plant Material and Growth Conditions

All Arabidopsis (*Arabidopsis thaliana*) lines used in this study were of the Wassilewskija (WS)-O ecotype. Seeds were surface sterilized using 30% bleach solution and stratified for 3 d in 0.15% agar at 4°C. For phenotypic analysis and growth assays plants were exposed to light for 1 h and grown in either continuous light (200 mmol m^{-2} s^{-1}) or complete darkness at 22°C on plates containing 0.5× Murashige and Skoog mineral salts (Sigma) and 1% agar.

Identification of T-DNA Insertions in *UGT80A2* and *UGT80B1*

Homozygous T-DNA insertion mutations in both *UGT80A2* and *UGT80B1* were identified by screening the Wisconsin T-DNA collection by PCR as described in Sussman et al. (2000). Screening primers for *UGT80A2* result in amplification of 440- and 581-bp products in mutant and wild type, respectively, with T-DNA primers JL214 5′-GCTGCGGACATCTACATTTTTG-3′, *UGT80A2*H245rev 5′-CTTCCCTGCAGAGATTTTGTCA-3′, and *UGT80A2*H245con 5′-ACGCATACGCAAATTCGAGATA-3′. Screening primers for *UGT80B1* result in 595- and 455-bp mutant and wild-type products using T-DNA primer JL214 5′-GCTGCGGACATCTACATTTTTG-3′, *UGT80B1*rev 5′-ATTGGCATTGAGAAAGGTTAGAG-3′, and *UGT80B1*con 5′-AGAATTGTGAAGTGGGTGATGG-3′. A 55°C annealing temperature was applied. Homozygous lines for *ugt80A2* and *ugt80B1* were crossed and F_2 progeny were screened for homozygous T-DNA insertions in both alleles.

SEM

All imaging was performed on a Quanta 200 (FEI Company) scanning electron microscope fit with a 1,000-mm gaseous secondary electron detector. Whole-seed specimens were mounted in cryo gel (Ted Pella, Inc.) on a temperature-controlled stage set at 1°C and pressure was maintained at 652 Pa. Image annotation and linear contrast optimization was performed in Adobe Illustrator CS2.

TEM

For analysis of mature seeds, seeds were dried after release from siliques. The seeds were placed at 4°C for 24 h in a 10 μM solution of abscisic acid to hydrate the seeds without inducing germination. Young seeds were extracted from immature siliques and were exposed to tetrazolium salts. Wild-type seeds that resisted staining with the salts and mutant seeds of an identical time point were selected for further electron microscopy processing. All fixation and embedding steps were performed through microwave processing. Samples were fixed in glutaraldehyde and dehydrated with ethanol increasing the concentration by 10% up to 100%. They were then infiltrated with a resin acetone mixture in steps of 1 part resin 2 parts acetone, 1 part resin 1 part acetone, and 2 parts resin 1 part acetone, after which the samples were polymerized in 100% resin overnight in 55°C. The samples were then

mounted, sectioned, and stained using 2% uranyl acetate in methanol and imaged with a Tecnai 12 TEM (FEI).

Histochemical Analysis

Tetrazolium Salt Uptake

Ability of seeds to uptake salt was tested by placing whole seeds in an aqueous solution of 1% (w/v) tetrazolium red (2,3,5-triphenyltetrazolium) at 30°C for 4 to 24 h. Seeds were removed from the solution and imaged by light microscopy.

Ruthenium Red

Ruthenium red (Sigma) was dissolved in water at a concentration of 0.03% (w/v) and seeds from wild type and mutants were imbibed in this solution for 30 min at 25°C. Seeds were removed from the imbibition solution and observed under a light microscope (Debeaujon et al., 2001, 2003).

DPBA

Seedlings were stained for 15 min using saturated (0.25%, w/v) DPBA with 0.005% (v/v) Triton X-100 and were visualized with an epifluorescent microscope equipped with a fluorescein isothiocyanate filter (excitation 450–490 nm, suppression LP 515 nm).

DMACA

Seeds were stained with DMACA reagent (2% [w/v] DMACA in 3 M HCl/50% [w/v] methanol) for one week, and then washed three times with 70% (v/v) ethanol. The stained pools were then examined using light microscopy.

Ultraviolet-Induced Fluorescence Analysis of Suberin Localized at the Seed Hilum

Seeds from wild-type WS-O, *ugt80A2*, *ugt80B1*, and the double mutant were examined under UV illumination for analysis of characteristic autofluorescence in the region of the seed hilum, reflecting suberin deposition (Beisson et al., 2007). Individual specimens were visualized under UV fluorescence using a compound microscope (Leitz DMRB, Leica).

Sterol Analysis

Sterols and sterol conjugates steryls (SEs, SG, and ASG) were isolated from wild-type, *ugt80A2*, *ugt80B1*, and double-mutant plant tissues. Briefly, the dried plant material was ground with a blender in a mixture of dichloromethane/methanol (2:1, v/v). Metabolites were extracted under reflux at 70°C. The dried residue was separated by thin-layer chromatography (Merck F254 0.25-mm thickness silica plates) using dichloromethane/methanol/water (85:15:0.5, v/v/v) as developing solvent (one run) and authentic standards as mobility references. SE, FSs, SG, and ASG were scraped off the plates. The dried residues of SE were saponified in methanolic KOH (6%) under reflux at 90°C for 1 h. The dried residues of SG or ASG were submitted to an acidic hydrolysis in an ethanolic solution of sulfuric acid (1%). Sterols were extracted from hydrolysates after addition of half a volume of water with 3 times 1 volume of *n*-hexane. Dried residues were subjected to an acetylation reaction for 1 h at 70°C with a mixture of pyridine/acetic anhydride/toluene (1:1:1, v/v/v). After evaporation of the reagents, steryl acetates were resolved as one band in a thin-layer chromatography using dichloromethane as developing solvent. Steryl acetates were analyzed and quantified in GC-flame ionization detector (FID) using cholesterol as an internal standard. Structures were confirmed by GC-MS.

Cell Wall Preparation and Analysis

Alditol acetate derivatives of the neutral sugars were measured on ball-milled (2 h) 4-week-old primary stem tissue. Cellulose contents were measured colorimetrically and total uronic acid content was determined by GC using 500 mg (dry weight) of ball-milled material as described (Blumenkranz and Asboe-Hanson, 1973; McCann et al., 1997).

Analysis of Seed Lipid Polyesters

Soluble lipids were removed from 250 to 350 mg mature seeds using the procedure described by Molina et al. (2006). The dry residue was depolymerized using acid-catalyzed methanolysis (5% [v/v] sulfuric acid in methanol for 2 h at 85°C). C17:0 methyl ester and C15 ω-pentadecalactone were used as internal standards. Monomers were extracted with 2 volumes of dichloromethane and 1 volume of 0.9% (w/v) NaCl. After aqueous washing, the organic phase was dried over anhydrous sodium sulfate and evaporated under nitrogen gas. The monomers were derivatized by acetylation or sylilation and separated, identified, and quantified by GS-MS. Splitless injection was used, and the mass spectrometer was run in scan mode over 40 to 500 atomic mass units (electron impact ionization), with peaks quantified on the basis of their total ion current. Details of chromatographic conditions and aliphatic and aromatic monomer identifications are described in Molina et al. (2006).

Whole Mounts of Embryos

Whole-mount preparations were done by clearing ovules from wild type and mutants in chloral hydrate solution made from an 8:3:1 mixture of chloral hydrate,water, and glycerol. Ovules were pooled from siliques into drops of chloral hydrate solution on microscope slides, followed by 24-h incubation at room temperature. Histological analysis and microscopy of ovules were performed with a Zeiss Axioskop 2. Digital images of embryos were captured with an AxioCam HRc with AxioVision Rel 4.3 software (Carl Zeiss GmbH). Images were processed with Adobe Photoshop 8.0 and Illustrator 11.0.0 software (Adobe Systems Inc.).

Sequence data from this article can be found in the GenBank/EMBL data libraries under accession numbers AY079032 (UGT80A2, AT3G07020) and BT005834 (UGT80B1, AT1G43620).

Supplemental Data

The following materials are available in the online version of this article.

Supplemental Figure S1. PCR confirmation of T-DNA insertion.

Supplemental Figure S2. Growth curves for *ugt80A2*, *ugt80B1*, and double mutant relative to wild type.

Supplemental Figure S3. Electrolyte leakage.

Supplemental Figure S4. Promoter::GUS fusion for UGT80A2.

Supplemental Figure S5. Promoter::GUS fusion for UGT80B1.

Supplemental Figure S6. Analysis of seed weight.

Supplemental Figure S7. Irregular DPBA and iodine staining of mutant cotyledons.

Supplemental Table S1. SG and ASG levels are reduced in *ugt80A2* and *ugt80B1* mutants.

Supplemental Materials and Methods S1.

ACKNOWLEDGMENTS

We thank Elliot Meyerowitz (California Institute of Technology), Cindy Cordova, Grace Qi (Keck Graduate Institute), and Darby Harris (University of Kentucky) for technical assistance, and Dirk Warneke (University of Hamburg) and Chris Shaw (University of British Columbia) for helpful discussion.

Received April 29, 2009; accepted July 20, 2009; published July 29, 2009.

LITERATURE CITED

Abraham W, Wertz PW, Burken RR, Downing DT (1987) Glucosylsterol and acylglucosylsterol of snake epidermis: structure determination. J Lipid Res **28:** 446–449

Baxter IR, Young JC, Armstrong G, Foster N, Bogenschutz N, Cordova T, Peer WA, Hazen SP, Murphy AS, Harper JF (2005) A plasma membrane H+-ATPase is required for the formation of proanthocyanidins in the seed coat endothelium of Arabidopsis thaliana. Proc Natl Acad Sci USA **102:** 2649–2654

Beisson F, Li YH, Bonaventure G, Pollard M, Ohlrogge JB (2007) The acyltransferase GPAT5 is required for the synthesis of suberin in seed coat and root of *Arabidopsis*. Plant Cell **19:** 351–368

Blumenkranz N, Asboe-Hanson G (1973) New methods for quantitative determination of uronic acids. Anal Biochem **54:** 484–489

Bouvier-Nave P, Ullmann P, Rimmele D, Benveniste P (1984) Phospholipid dependence of plant UDP-glucose sterol β-D-glucosyl transferase. I. Detergent mediated delipidation by selective solubilization. Plant Sci Lett **36:** 19–27

Bretscher MS, Munro S (1993) Cholesterol and the Golgi-apparatus. Science **261:** 1280–1281

Cruz-Aguado R, Shaw CA (2009) The ALS/PDC syndrome of Guam and the cycad hypothesis. Neurology **72:** 474–476

Debeaujon I, Nesi N, Perez P, Devic M, Grandjean O, Caboche M, Lepiniec L (2003) Proanthocyanidin-accumulating cells in *Arabidopsis* testa: regulation of differentiation and role in seed development. Plant Cell **15:** 2514–2531

Debeaujon I, Peeters AJM, Leon-Kloosterziel KM, Koornneef M (2001) The TRANSPARENT TESTA12 gene of *Arabidopsis* encodes a multidrug secondary transporter-like protein required for flavonoid sequestration in vacuoles of the seed coat endothelium. Plant Cell **13:** 853–871

DeBolt S, Gutierrez R, Ehrhardt DW, Somerville C (2007) Nonmotile cellulose synthase subunits repeatedly accumulate within localized regions at the plasma membrane in Arabidopsis hypocotyl cells following 2,6-dichlorobenzonitrile treatment. Plant Physiol **145:** 334–338

Esders TW, Light RJ (1972) Characterization and in vivo production of three glycolipids from Candida bogoriensis: 13-glucopyranosylglucopyranosyloxydocosanoic acid and its mono- and diacetylated derivatives. J Lipid Res **13:** 663–671

Focks N, Sagasser M, Weisshaar B, Benning C (1999) Characterization of tt15, a novel transparent testa mutant of Arabidopsis thaliana (L.) Heynh. Planta **208:** 352–357

Frasch W, Grunwald C (1976) Acylated steryl glycoside synthesis in seedlings of *Nicotiana tabacum* L. Plant Physiol **58:** 744–748

Grunwald C (1978) Steryl glycoside biosynthesis. Lipids **13:** 697–703

Haque M, Hirai Y, Yokota K, Mori N, Jahan I, Ito H, Hotta H, Yano I, Kanemasa Y, Oguma K (1996) Lipid profile of Helicobacter spp.: presence of cholesteryl glucoside as a characteristic feature. J Bacteriol **178:** 2065–2070

Hartmann-Bouillon MA, Benveniste P (1978) Sterol biosynthetic capacity of purified membrane fractions from maize coleoptiles. Phytochemistry **17:** 1037–1042

Hillig I, Leipelt M, Ott C, Zahringer U, Warnecke D, Heinz E (2003) Formation of glucosylceramide and sterol glucoside by a UDP-glucose-dependent glucosylceramide synthase from cotton expressed in Pichia pastoris. FEBS Lett **553:** 365–369

Iribarren M, Pomilio AB (1985) Sitosterol 3-O-[alpha]-riburonofuranoside from Bauhinia candicans. Phytochemistry **24:** 360–361

Jez JM, Bowman ME, Dixon RA, Noel JP (2000) Structure and mechanism of the evolutionarily unique plant enzyme chalcone isomerase. Nat Struct Biol **7:** 786–791

Kojima M, Ohnishi M, Ito S, Fujino Y (1989) Characterization of acylmonoglycosylsterol, monoglycosylsterol, diglycosylsterol, triglycosylsterol, tetraglycosylsterol and saponin in Adzuki bean (Vigna angularis) seeds. Lipids **24:** 849–853

Kunimoto S, Kobayashi T, Kobayashi S, Murakami-Murofushi K (2000) Expression of cholesteryl glucoside by heat shock in human fibroblasts. Cell Stress Chaperones **5:** 3–7

Lepage M (1964) Isolation and characterization of an esterified form of steryl glucoside. J Lipid Res **5:** 587–592

Li YH, Beisson F, Koo AJK, Molina I, Pollard M, Ohlrogge JB (2007) Identification of acyltransferases required for cutin biosynthesis and production of cutin with suberin-like monomers. Proc Natl Acad Sci USA **104:** 18339–18344

Ly PTT, Singh S, Shaw CA (2007) Novel environmental toxins: steryl glycosides as a potential etiological factor for age-related neurodegenerative diseases. J Neurosci Res **85:** 231–237

Mayberry WR, Smith PF (1983) Structures and properties of acyl diglucosylcholesterol and galactofuranosyl diacyglycerol from Acholeplasma axanthum. Biochim Biophys Acta **752:** 434–443

McCann M, Chen L, Roberts K, Kemsley E, Sene C, Carpita N, Stacey N, Wilson R (1997) Infrared microspectroscopy: sampling heterogeneity in plant cell wall composition and architecture. Physiol Plant **100:** 729–738

Molina I, Bonaventure G, Ohlrogge J, Pollard M (2006) The lipid polyester composition of *Arabidopsis thaliana* and *Brassica napus* seeds. Phytochemistry **67:** 2597–2610

Molina I, Ohlrogge JB, Pollard M (2008) Deposition and localization of lipid polyester in developing seeds of Brassica napus and Arabidopsis thaliana. Plant J **53:** 437–449

Murakami-Murofushi K, Nakamura K, Ohta J, Suzuki M, Suzuki A, Murofushi H, Yokota T (1987) Expression of poriferasterol monoglucoside associated with differentiation of Physarum polycephalum. J Biol Chem **262:** 16719–16723

Palta JP, Whitaker BD, Weiss LS (1993) Plasma membrane lipids associated with genetic variability in freezing tolerance and cold acclimation of Solanum species. Plant Physiol **103:** 793–803

Patterson GW, Hugly S, Harrison D (1993) Sterols and phytyl esters of Arabidopsis thaliana under normal and chilling temperatures. Phytochemistry **33:** 1381–1383

Peng LC, Kawagoe Y, Hogan P, Delmer D (2002) Sitosterol-beta-glucoside as primer for cellulose synthesis in plants. Science **295:** 147–150

Pollard M, Beisson F, Li Y, Ohlrogge JB (2008) Building lipid barriers: biosynthesis of cutin and suberin. Trends Plant Sci **13:** 236–246

Schaller H (2003) The role of sterols in plant growth and development. Prog Lipid Res **42:** 163–175

Schrick K, Fujioka S, Takatsuto S, Stierhof YD, Stransky H, Yoshida S, Jurgens G (2004) A link between sterol biosynthesis, the cell wall, and cellulose in Arabidopsis. Plant J **38:** 227–243

Sussman MR, Amasino RM, Young JC, Krysan PJ, Austin-Phillips S (2000) The Arabidopsis knockout facility at the University of Wisconsin-Madison. Plant Physiol **124:** 1465–1467

Ullmann P, Bouvier-Nave P, Benveniste P (1987) Regulation by phospholipids and kinetic studies of plant membrane bound UDP-glucose sterol β-D-glucosyl transferase. Plant Physiol **85:** 51–55

Ury A, Benveniste P, Bouvier-Nave P (1989) Phospholipid dependence of plant UDP-glucose sterol β-D-glucosyl transferase. Plant Physiol **91:** 567–573

Warnecke D, Erdmann R, Fahl A, Hube B, Muller F, Zank T, Zahringer U, Heinz E (1999) Cloning and functional expression of UGT genes encoding sterol glucosyltransferases from *Saccharomyces cerevisiae*, *Candida albicans*, *Pichia pastoris*, and *Dictyostelium discoideum*. J Biol Chem **274:** 13048–13059

Warnecke DC, Baltrusch M, Buck F, Wolter FP, Heinz E (1997) UDP-glucose:sterol glucosyltransferase: cloning and functional expression in Escherichia coli. Plant Mol Biol **35:** 597–603

Warnecke DC, Heinz E (1994) Purification of a membrane-bound UDP-glucose:sterol β-D-glucosyltransferase based on its solubility in diethyl ether. Plant Physiol **105:** 1067–1073

Yoshida S, Uemura M (1986) Lipid composition of plasma membranes and tonoplasts isolated from etiolated seedlings of mung bean (*Vigna radiata* L.). Plant Physiol **82:** 807–812